Remarkably Size-Regulated Cell Invasion by Artificial Viruses. Saccharide-Dependent Self-Aggregation of Glycoviruses and Its Consequences in Glycoviral Gene Delivery

Takashi Nakai, Takuya Kanamori, Shinsuke Sando, and Yasuhiro Aoyama*

Contribution from the Department of Synthetic Chemistry and Biological Chemistry, Graduate School of Engineering, Kyoto University, Yoshida, Sakyo-ku, Kyoto 606-8501, Japan

Received April 15, 2003; E-mail: aoyamay@sbchem.kyoto-u.ac.jp

Abstract: We here report a novel example of artificial glycoviral vectors constructed via number- and size-controlled gene (pCMVluc, 7040 bp) coating with micellar glycocluster nanoparticles (GNPs) of calix[4]-resorcarene-based macrocyclic glycocluster amphiphiles having eight or five saccharide moieties with terminal α-glucose (α-Glc), β-glucose (β-Glc), or β-galactose (β-Gal) residues. The resulting glycoviruses are compactly packed (∼50 nm) and well charge-shielded ($\zeta \cong 0$ mV), undergo saccharide-dependent (α-Glc > β-Gal ≫ β-Glc) self-aggregation, and transfect cell (Hela and HepG2) cultures as triggered by the pinocytic form of endocytosis. The semilogarithmic linear size–activity correlation suggests that size-restricted pinocytosis (<100 nm) is effective only for monomeric viruses. The activities of oligomeric and otherwise poorly active β-Gal-functionalized viruses toward hepatic HepG2 cells are ∼10^2-times higher than expected on the size basis, owing to the receptor-mediated specific pathway involving the asialoglycoprotein receptors on the hepatic cell surfaces. The scope and prospect of artificial glycoviruses are discussed.

Introduction

Viruses owe their use in gene delivery to their intrinsic function, that is, cell invasion followed by gene expression.[1] Their therapeutic performance, however, is still not satisfactory.[2] There has also been an intense recent concern about amine-based cationic polymers/dendrimers and lipid aggregates (the so-called cationic liposomes) as nonviral vectors.[3,4] Their merit is at least dual. They readily form complexes with polyanionic DNAs on an electrostatic basis[5] and the amine functionalities are easily modifiable so as to present specific ligands for targeting particular cell types, a typical example being galactose for hepatic (liver) cells.[4a,6,7] At the same time, the ease of amine–DNA complexation obscures the stoichiometry thereof. More accurately, polycation–polyanion amine–DNA complexes can exist at least apparently in various amine/DNA or N/P ratios.[8] In addition, they often undergo cross-link and further aggregation upon charge neutralization,[9] giving rise to poly-

molecular (with respect to DNA)[10] and huge (even μm-sized) particles.[11] With this being the case, a couple of problems arise. One is that the composition and size of DNA-bearing aggregates could change from system to system, upon ligand modification, and with varying N/P's even within a given system.[6w,12] The in vitro transfection efficiencies and selectivities are indeed N/P-dependent[6n,q,t,w,x] and hence less uniquely definable; comparison between different systems becomes less meaningful unless size factors[13] are adequately taken into account. The other problem associated with big particles in vivo is their size-restricted poor diffusion in vascular periphery. Size may also be a governing factor of transfection itself,[13] since it is triggered by cellular uptake of DNA-bearing particles usually via size-restricted endocytosis.[14]

The term "artificial virus" has been occasionally used for cationic vectors mimicking some characteristic aspects of viral

(1) (a) Wilson, J. M. *New Engl. J. Med.* **1996**, *334*, 1185−1187.
(2) (a) Verma, I. M.; Somia, N. *Nature* **1997**, *389*, 239−242. (b) Anderson, W. L. *Nature* **1998**, *392*, 25−30. (c) Yla-Herttuala, S.; Martin, J. F. *Lancet* **2000**, *355*, 213−222.
(3) (a) *Self-assembling Complexes for Gene Delivery. From Laboratory to Clinical Trial*; Kabanov, A. V., Felgner, P. L., Seymour, L. W., Eds.; Wiley: Chichester, 1998. (b) Behr, J.-P. *Acc. Chem. Res.* **1993**, *26*, 274−278. (c) Nguyen, H.-K.; Lemieux, P.; Vinogradov, S. V.; Gebhart, C. L.; Guérin, N.; Paradis, G.; Bronich, T. K.; Alakhov, V. Y.; Kabanov, A. V. *Gene Ther.* **2000**, *7*, 126−138. (d) Han, S.-O.; Mahato, R. I.; Sung, Y. K.; Kim, S. W. *Mol. Ther.* **2000**, *2*, 302−317. (e) Nishikawa, M.; Huang, L. *Hum. Gene. Ther.* **2001**, *12*, 861−870. (f) Zuber, G.; Dauty, E.; Nothisen, M.; Berguise, P.; Behr, J.-P. *Adv. Drug. Delivery Rev.* **2001**, *52*, 245−253. (g) Gebhart, C. L.; Kabanov, A. V. *J. Cont. Relat.* **2001**, *73*, 401−416. (h) Ogris. M.; Wagner, E. *Drug Discovery Today* **2002**, *7*, 479−485. (i) Wolff, J. A. *Nature Biotechnol.* **2002**, *20*, 768−769. (j) Niidome, T.; Huang, L. *Gene Ther.* **2002**, *9*, 1647−1652.
(4) (a) Wu, G. Y.; Wu, C. H. *J. Biol. Chem.* **1987**, *262*, 4429−4432. (b) Felgner, P. L.; Tsai, Y. J.; Sukhu, L.; Wheeler, C. J.; Manthorpe, M.; Marshall, J.; Cheng, S. H. *Proc. Natl. Acad. Sic. U.S.A.* **1987**, *84*, 7413−7417. (c) Felgner, P. L.; Tsai, Y. J.; Sukhu, L.; Wheeler, C. J.; Manthorpe, M.; Marshall, J.; Cheng, S. H. *Ann. N.Y. Acad. Sci.* **1995**, *772*, 126−139. (d) Cao, X.; Hunag, L. *Gene Ther.* **1995**, *2*, 710−722. (e) Tang, M. X.; Redemann, C. T.; Szoka, F. C. *Bioconjugate Chem.* **1996**, *7*, 703−714. (f) Lim, Y.-B.; Choi, Y. H.; Park, J.-S. *J. Am. Chem. Soc.* **1999**, *121*, 5633−5639. (g) Lim, Y.-B.; Kim, C.-H.; Kim, K.; Kim, S.-W.; Park, J.-S. *J. Am. Chem. Soc.* **2000**, *122*, 6524−6525. (h) Bronich, T. K.; Nguyen, H. K.; Eisenberg, A.; Kabanov, A. V. *J. Am. Chem. Soc.* **2000**, *122*, 8339−8343. (i) Putnam, D.; Gentry, C. A.; Pack, D. W.; Langer, R. *Proc. Natl. Acad. Sci. U.S.A.* **2001**, *98*, 1200−1205. (j) Lim, Y.-B.; Kim, S.-M.; Lee, Y.; Lee, W.-K.; Yang, T.-G.; Lee, M.-J. Suh, H.; Park, J.-S. *J. Am. Chem. Soc.* **2001**, *123*, 2460−2461. (k) Lynn, D. M.; Anderson, D. G.; Putnam, D.; Langer, R. *J. Am. Chem. Soc.* **2001**, *123*, 8155−8156.
(5) (a) Labat-Moleur, F.; Steffan, A. M.; Brisson, C.; Perron, H.; Feugeas, O.; Furstenberger, P.; Oberling, F.; Brambilla, E.; Behr, J.-P. *Gene Ther.* **1996**, *3*, 1010−1017. (b) Mislick, K. A.; Baldeschwieler, J. D. *Proc. Natl. Acad. Sci. U.S.A.* **1996**, *93*, 12349−12354.

vectors.[15] Viruses contain a single genetic (DNA or RNA) molecule which is coated with many but a very definite number of capsid proteins in a compact viral size (20−100 nm). Monomolecularity, stoichiometry, and size in addition to transfection ability are the criteria for artificial viruses here. Our

(6) (a) Wu, G. Y.; Wu, C. H. *J. Biol. Chem.* **1988**, *263*, 14621−14624. (b) Plank, C.; Zatloukal, K.; Cotton, M.; Mechtler, K.; Wagner, E. *Bioconjugate Chem.* **1992**, 3, 533−539. (c) Midoux, P.; Mendes, C.; Legrand, A.; Raimond, J.; Mayer, R.; Monsugny, M.; Roche, A. C. *Nucleic Acids Res.* **1993**, *21*, 871−878. (d) Ledley, F. D. *Hepatology* **1993**, *18*, 1263−1273. (e) Cristiano, R. J.; Smith, L. C.; Woo, S. L. C. *Proc. Natl. Acad. Sci. U.S.A.* **1993**, *90*, 2122−2126. (f) Frese, J.; Wu, C. H.; Wu, J. Y. *Adv. Drug Delivery Rev.* **1994**, *14*, 137−152. (g) Chen, J.; Stickles, R. J.; Daichendt, K. A. *Hum. Gene Ther.* **1994**, *5*, 429−435. (h) Merwin, J. R.; Noell, G. S.; Thomas, W. L.; Chiou, H. C.; Derome, M. E.; McKee, T. D.; Spitalny, G. L.; Findeis, M. A. *Bioconjugate Chem.* **1994**, *5*, 612−620. (i) Perales, J. C.; Ferkol, T.; Beegen, H. Ratnoff, O. D.; Hanson, R. W.; *Proc. Natl. Acad. Sci. U.S.A.* **1994**, *91*, 4086−4090. (j) Wadhwa, M. S.; Knoell, D. L.; Young, A. P.; Rice, K. G. *Bioconjugate Chem.* **1995**, *6*, 283−291. (k) Remy, J.-S.; Kichler, A.; Mordvinov, V.; Schuber, F.; Behr, J.-P. *Proc. Natl. Acad. Sci. U.S.A.* **1995**, *92*, 1744−1748. (l) Erbacher, P.; Bousser, M.-T.; Raimond, J.; Monsigny, M.; Midoux, P. Roche, A. C. *Hum. Gene Ther.* **1996**, *7*, 721−729. (m) Perales, J. C.; Grossman, G. A.; Molas, M.; Liu, G.; Felkol, T.; Harpst, J.; Oda, H.; Hanson, R. W. *J. Biol. Chem.* **1997**, *272*, 7398−7407. (n) Zanta, M.-A.; Boussif, O.; Adib, A.; Behr, J.-P. *Bioconjugate. Chem.* **1997**, *8*, 839−844. (o) Choi, H. Y.; Liu, F.; Park, J. S.; Kim, S. W. *Bioconjugate Chem.* **1998**, *9*, 708−718. (p) Chemin, I.; Moradpour, D.; Wieland, S.; Offensperger, W.-B.; Walter, E.; Behr, J.-P.; Blum, H. E. *J. Viral Hepatitis* **1998**, *5*, 369−375. (q) Kawakami, S.; Yamashita, F.; Nishikawa, M.; Takakura, Y.; Hashida, M. *Biochem. Biophys. Res. Commun.* **1998**, *252*, 78−83. (r) Hashida, M.; Takemura, S.; Nishikawa, M.; Takakura, Y. J. *J. Controlled Release* **1998**, *53*, 301−310. (s) Han, J.; Lim, M.; Yeom, Y. J. *Biol. Pharm. Bull.* **1999**, *22*, 836−840. (t) Bettinger, T.; Remy, J.-S.; Erbacher, P. *Bioconjugate Chem.* **1999**, *10*, 558−561. (u) Nishikawa, M.; Yamauchi, M.; Morimoto, K.; Ishida, E.; Takakura, Y.; Hashida, M. *Gene Ther.* **2000**, *7*, 548−555. (v) Niidome, T.; Urakawa, M.; Sato, H.; Takahara, Y.; Anai, T.; Hatakayama, T.; Wada, A.; Hirayama, T.; Aoyagi, H. *Biomaterials* **2000**, *21*, 1811−1819. (w) Park, I. K.; Kim, T. H.; Park, Y. H.; Shin, B. A.; Choi, E. S.; Chowdhury, E. H.; Akaike, T.; Cho, C. S. *J. Controlled Release* **2001**, *76*, 349−362. (x) Gaucheron, J.; Santaella, C.; Vierling, P. *Bioconjugate Chem.* **2001**, *12*, 569−575.

(7) For targeted gene delivery to cells other than hepatic, see: (a) Buschle, M. Cotton, M.; Kirlappos, H.; Mechtler, K.; Schffner, G.; Zauner, W.; Birnstiel, M. L.; Wagner, E. *Hum. Gene Ther.* **1995**, *6*, 753−761. (b) Ferkol, T.; Perales, J. C.; Muralo, F.; Hanson, R. W. *Proc. Natl. Acad. Sci. U.S.A.* **1996**, *93*, 101−105. (c) Kiecheis, R.; Kichler, A.; Kursa, M.; Ogris, M.; Felzmann, T.; Buchberger, M.; Wagner, E. *Gene Ther.* **1997**, *4*, 409−418. (d) Uherek, C.; Wels, W. *Adv. Drug Delivey Rev.* **2000**, *44*, 153−166. (e) Yu, L.; Nielsen, M.; Han, S.-O.; Kim, S. W. *J. Controlled Release.* **2001**, *72*, 179−189. (f) Gaidamakova, E. K.; Backer, M. V.; Backer, J. M. *J. Controlled Release* **2001**, *74*, 341−347. (g) Ogris, M.; Wagner, E. *Drug Discovery Today* **2002**, *20*, 768−769. (h) Dauty, E.; Remy, J.-S.; Zuber, G.; Behr, J.-P. *Bioconjugate Chem.* **2002**, *13*, 831−839. (i) Hood, J. D.; Bednarski, M.; Frausto, R.; Guccione, S.; Reisfeld, R. A.; Xiang, R.; Cheresh, D. A. *Science* **2002**, *296*, 2404−2407. (j) Niethammer, A. G.; Xiang, R.; Becker, J. C.; Wodrich, H.; Pertl, U.; Karsten, G.; Eliceiri, B. P.; Reisfeld, R. A. *Nat. Med. (N.Y.)* **2002**, *8*, 1369−1375.

(8) For polyamine−DNA complexes with defined stoichiometry, see, for example: Kabanov, A. V.; Kabanov, V. A. *Bioconjugate Chem.* **1995**, *6*, 7−20.

(9) Jaaskelainen, I.; Monkkonen, J.; Urtti, A. *Biochim. Biophys. Acta* **1994**, *1195*, 115−123.

(10) Tang, M. X.; Szoka, F. C. *Gene Ther.* **1997**, *4*, 823−832.

(11) (a) Zabner, J.; Fasbender, A. J.; Moninger, T.; Poellinger, K. A.; Welsh, M. J. *J. Biol. Chem.* **1995**, *270*, 18997−19007. (b) Xu, Y.; Szoka, F. C. *Biochemistry* **1996**, *35*, 5616−5623.

(12) Dauty, E.; Remy, J.-S.; Blessing, T.; Behr, J.-P. *J. Am. Chem. Soc.* **2001**, *123*, 9227−9234.

(13) (a) Kabanov, A. V.; Szoka, F. C.; Seymour, L. W. *Self-assembling Complexes for Gene Delivery. From Laboratory to Clinical Trial*; Kabanov, A. V., Felgner, P. L., Seymour, L. W., Eds.; Wiley: Chichester, 1998; Chapter 10, pp 197−218. (b) Zhou, X.; Klibanov, A. L.; Huang, L. *Biochim. Biophys. Acta* **1991**, *1065*, 8−14. (c) Wagner, E.; Cotten, M.; Foisner, R.; Birnstiel, M. L. *Proc. Natl. Acad. Sci. U.S.A.* **1991**, *88*, 4255−4259. (d) Sukhishvili, S. A.; Obolskii, O. L.; Astafieva, I. V.; Kabanov, A. V.; Yaroslavov, A. A. *Polym. Sci.* **1993**, *35*, 1602−1606. (e) Kabanov, A. V.; Kabanov, V. A. *Bioconjugate Chem.* **1995**, *6*, 7−20. (f) Boussif, O.; Leozoulalc′h, F.; Zanta, M. A.; Mergny, M. D.; Scherman, D.; Demeniex, B.; Behr, J.-P. *Proc. Natl. Acad. Sci. U.S.A.* **1995**, *92*, 7297−7301. (g) Wolfert, M. A.; Seymour, L. W. *Gene Ther.* **1996**, *3*, 269−273. (h) Cherng, J.-Y.; van de Weterling, P.; Herre, T.; Crommelin, D. J. A.; Hennink, W. E. *Pharm. Res.* **1996**, *13*, 1038−1042. (i) Reference 10.

(14) Depending on the size of endocytic vesicles, endocytosis is classified into two categories, pinocytosis (cellular drinking) and phagocytosis (cellular eating), by which guest objects are accommodated in picocytic vesicles (~100 nm) and phagocytic vesicles (>250 nm), respectively: Alberts, B.; Johnson, A.; Lewis, J.; Raff, M.; Roberts, K.; Walter, P. *Molecular Biology of Cell* (4th ed.); Garland Science: New York, 2002; Chapter 13, p 746.

strategy is to coat DNA with neutral glycocluster nanoparticles,[16] whose uncharged and highly hydrophilic surfaces would prevent the resulting glycoviruses from aggregation. The first member of this family, derived from disaccharide cellobiose, indeed meets all the above criteria.[17] The present work is concerned about alteration in saccharides, where we unexpectedly find that the glycoviruses undergo saccharide-dependent self-aggregation. The object of this work is to extract pure size effects and pure receptor contributions in the absence of complication arising from the charge effects. We report here that the size effects in the present glycoviral gene delivery are such that allow only monomeric viruses to work effectively and a size-corrected factor of ~10^2 can be assigned to the receptor-mediated hepatocyte targeting by the galactose-functionalized viruses.

Experimental Section

Gly8 and Gly5. Gly8 compounds (Gly8, Cel8, and Lac8) were obtained as described.[18] In the particular preparation in this work, we slowly added a methanol solution (5 mL) of octaamine **1** (200 mg, 0.14 mmol) to an ethanol solution (40 mL) of maltonolactone, cellobiolactone, or lactonolactone (1.52 g, 4.48 mmol) under nitrogen. The mixture was stirred at 25 °C for 8 h. White precipitates which separated upon cooling the solution with ice were collected by filtration, washed twice with cold methanol, dissolved in water, reprecipitated upon addition of methanol after filtration of the aqueous solution through a membrane filter (Sterile Acrodisk 25, Gelman Science, pore size 0.45 μm), and freeze-dried to give Mal8, Cel8, or Lac8 (400−460 mg, 70−80%).

Gly5 counterparts (Mal5, Cel5, and Lac5) were prepared by using a controlled amount (5−7 equiv) of lactone. Into an ethanol solution (20 mL) of octaamine **1** (250 mg, 0.17 mmol) was slowly added a methanol solution (10 mL) of a lactone (290−400 mg, 0.85−1.2 mmol) under nitrogen. The mixture was stirred at 25 °C for 20 h. The Gly5 products obtained by following the same workup procedure as above were checked by elemental analysis with C/N as an index (C/N = 15.86 for Gly5, 19.71 for Gly8, and 9.43 for unsubstituted octaamine **1**). The amount of lactone was varied in the range of 5−7 equiv so as to give the best fit to the required C/N of 15.86. The actual Gly5 samples used here had C/N = 16.00 (Mal5), 16.34 (Cel5), or 16.12 (Lac5), corresponding to Mal5.1, Cel5.4, or Lac5.2, respectively. They showed satisfactory ^{1}H NMR spectra. The yields were 178 mg (33%) for Mal5, 234 mg (43%) for Cel5, and 190 mg (35%) for Lac5.

Plasmid. Plasmid DNA pCMVluc was obtained by subcloning of the HindIII/XbaI firefly luciferase cDNA from pGL3-control vector

(15) For the approach to artificial viruses based on detergent or saccharide manipulation of cationic vectors to allow monomolecular DNA collapse, see: (a) Blessing, T.; Remy, J.-S.; Behr, J.-P. *Proc. Natl. Acad. Sci. U.S.A.* **1998**, *95*, 1427−1431. (b) Blessing, T.; Remy, J.-S.; Behr, J.-P. *J. Am. Chem. Soc.* **1998**, *120*, 8519−8520. (c) Bettinger, T.; Remy, J.-S.; Erbacher, P. *Bioconjugate Chem.* **1999**, *10*, 558−561. (d) Duaty, E.; Behr, J.-P.; Remy, J.-S. *Gene Ther.* **2002**, *9*, 743−748. (e) Zuber, G.; Dauty, E.; Nothisen, M.; Belguise, P.; Behr, J.-P. *Adv. Drug Delivery Rev.* **2001**, *52*, 245−25.

(16) Maltose cluster compound **2a** (Mal8) was found to form micellar glyco- cluster nanoparticles (GNPs) and to strongly interact with the phosphate ions of Na₂HPO₄ and DNA in water. These key observations led us to carry out the present work. For the detailed nature of GNP-forming irreversible micellization of amphihile **2a** (Mal8), its conformation in GNP, and phosphate−GNP interactions, see ref 16c. (a) Hayashida, O.; Kato, M.; Akagi, K.; Aoyama, Y. *J. Am. Chem. Soc.* **1999**, *121*, 11597−11598. (b) Hayashida, O.; Matsuo, A.; Aoyama, Y. *Chem. Lett.* **2001**, 272−273. (c) Hayashida, O.; Mizuki, K.; Akagi, K.; Matsuo, A.; Kanamori, T.; Nakai, T.; Sando, S.; Aoyama, Y. *J. Am. Chem. Soc.* **2003**, *125*, 594−601.

(17) Aoyama, Y.; Kanamori, T.; Nakai, T.; Sasaki, T.; Horiuchi, S. Sando, S.; Niidome, T. *J. Am. Chem. Soc.* **2003**, *125*, 3455−3457.

(18) For Mal8: (a) ref 16. (b) Fujimoto, T.; Shimizu, C.; Hayashida, O.; Aoyama, Y. *J. Am. Chem. Soc.* **1997**, *119*, 6676−6677. (c) Fujimoto, T.; Shimizu, C.; Hayashida, O.; Aoyama, Y. *J. Am. Chem. Soc.* **1997**, *120*, 6601−602. (d) Fujimoto, K.; Miyata, T.; Aoyama, Y. *J. Am. Chem. Soc.* **2000**, *122*, 3558−3559. For Cel8: ref 17. For Lac8: (a) Ref 16c for Mal8 above. (b) Fujimoto, T.; Shimizu, C.; Hayashida, O.; Aoyama, Y. *Gazz. Chim. Ital.* **1997**, *127*, 749−752.

(Promega) into the polylinker of the pcDNA3 vector (Invitrogen). pCMVluc was amplified in the *Escherichia coli* strain DH5α, isolated and purified using a QIAGEN Plasmid Mega kit (QIAGEN), and obtained as a TRIS-EDTA solution (>1 $\mu g/\mu L$). The purity of pCMVluc was checked by electrophoresis and also by referring to OD_{260}/OD_{280} > 1.8 (OD = optical density).

Fluorescence labeling of pCMVluc with tetramethylrhodamine on the guanine moieties was carried out as described in the protocol of label IT reagent (Mirus Corp.). The modified plasmid showed fluorescent bands in electrophoresis; the bands were otherwise indistinguishable from those of parent pCMVluc when stained by ethidium bromide.

General Analyses. Water was of an ultrapure grade. The concentrations of Gly8(5) and pCMVluc in buffer solution were based on $\epsilon_{282} = 15.8 \times 10^3$ $(M\ cm)^{-1}$ and $\epsilon_{260} = 127$ $(M\ base\ cm)^{-1}$, respectively. Gel permeation chromatography (GPC) for Gly8(5) was performed on a Showa Denko Shodex GPC-101 chromatograph using a Shodex Asahipak GS-320 QH packed column with water as an eluant at a flow rate of 0.5 mL/min. Molecular weights were calibrated with pullulan standards having a molecular weight of 5900, 11800, 22800, or 47300. Dynamic light scattering (DLS) measurements for Gly8(5) (1 mM) in water or for Gly8(5)−pCMVluc complexes (glycoviruses) (1 μM P with Gly8(5)/P = 0−2.0) in HEPES buffer (10 mM, pH 7.4, [NaCl] = 150 mM) were carried out with a Particle Sizing Systems NICOMP 380 ZLS zeta potential/particle sizer at 100 mW green laser at 532 nm. Zeta potentials of the complexes (50 μM P with Gly8(5)/P = 0.5−2.0) were obtained by using the same machine. TEM (transmission electron microscopy) images for Gly8(5) (1 mM) or for glycoviruses (50 μM P with Gly8(5)/P = 1.0) were taken on a JEOL JEM-1230 electron microscope at an acceleration voltage of 100 kV with uranyl acetate (3 wt %) or sodium phosphotungstate (2 wt %) as a negative stainer or uranyl acetate (0.6 wt %) or RuO_4 (vapor) as a positive stainer. A drop of a sample solution was applied on a hydrophilized, carbon-coated copper grid, and excess solution was removed by the help of filter paper. The grid was dipped in a stainer solution, removed of excess solution as above, air-dried, and then subjected to the measurements of microscopic images.

Cell Cultures. Hela cells (a human malignant uterine cell line) and HepG2 cells (a human malignant hepatic cell line) were purchased from Riken Cell Bank (RCB accession no. RCB0007) and Dainippon Pharmaceutical Co. Ltd. (ATCC accession no. HB8065), respectively, and were cultivated in DMEM (Dulbecco's modified Eagle's medium) containing 10% FBS (fetal bovine serum) and antibiotics (50 $\mu g/mL$ streptomycin) with (HepG2) or without (Hela) 1% NEAA (nonessential amino acids) at 37 °C in a humidified atmosphere containing 5% CO_2.

Hela cells with fluorescence-labeled endosomes were obtained by lipofection of the cells with plasmid pEGFP-Endo (Clontech Laboratories Inc.) encoding a gene for fused protein GFP-RhoB, in which green flurescent protein (GFP) is linked with the endosome-localized protein RhoB. Lipofection was carried out as described in the protocol of lipofectin reagent (Invitrogen Corp.).

Transfection. Cells (Hela or HepG2) were seeded at a density of 4.0×10^4 cells/well in a 24-well plate and cultivated. After 24 h, the cells became ∼20% confluent and were washed with 400 μL of a transfection medium, Opti-MEM (GIBCO). To the cells in each well was added a transfection solution (400 μL) prepared by mixing 100 μL of a solution of pCMVluc (6.0 $\mu g/mL$ or 18.2 μM P) in Opti-MEM, *x* μL (*x* = 0−100) of a solution (36.3 μM) of Gly8(5) in Opti-MEM, and $[400 - (100 + x)]$ μL of Opti-MEM; the final [pCMVluc] was 4.5 μM P or 0.6 μg of plasmid per well and Gly8(5)/P changed in the range of 0−2.0. After incubation for 6 h at 37 °C, the medium was replaced by 400 μL of fresh DMEM containing 10% FBS, and the cells were further incubated for 48 h. The luciferase assay was performed by the conventional chemiluminescence method using a Lumat LB9507 luminometer (Berthold Detection Systems) and the luciferase assay kit (Promega). Luciferase relative light units (RLU)

integrated over 10 s are normalized for the total protein content of the cell lysate, obtained by the Bradford assay (Bio-Rad Laboratories) using bovine serum alubumin as a standard.

For inhibition studies, cells were incubated in a cultivation (DMEM) medium containing cytochalasin B (50 μM) or wortmannin (10 μM) for 30 min. The medium was replaced by a glycovirus-containing Opti-MEM medium to start transfection. Asialofetuin (0.5 mg/mL), on the other hand, was simply added in a transfection medium.

For fluorescence microscopic studies, cells lipofected with pEGFP-Endo were cultivated on a cover glass for 6 h, during which the cell reached ∼70% confluent and became appropriately endosome-labeled. The medium was replaced by Opti-MEM containing fluorescence-labeled plasmid pCMVluc (1 $\mu g/mL$) and Cel8 at Cel8/P = 1.0. After incubation at either 37 or 4 °C for 30 min, the cover glass was recovered and the cells thereon were washed twice with phosphate buffer, immobilized with 2.5% glutaldehyde, and subjected to the measurements of fluorescence micrographs using an Olympus IX70 fluorescence microscope with an appropriate filter.

Results and Discussion

Glycocluster Nanoparticles (GNPs). The glycocluster compounds we use here are obtained by the reactions of macrocyclic octaamine **1** (R = $(CH_2)_{10}CH_3$) with a lactone derivative of 1,4-linked disaccharide maltose (glucosyl-α-glucose), cellobiose (glucosyl-β-glucose), or lactose (galactosyl-β-glucose). The common gluconolactone residue thereby undergoes ring-opening and is attached via amide linkage on the macrocycle with the α-glucose (α-Glc), β-glucose (β-Glc), or β-galactose (β-Gal) moiety in an intact pyranose form (Figure 1). The reaction proceeds smoothly; full substitution is readily achieved to give macrocyclic glycolipid-bundle type compounds (**2a**−**2c**) having eight saccharide moieties and four long alkyl (undecyl) chains on the opposite sides of the calix[4]resorcarene framework. The use of a limited amount of lactone (5−7 equiv) allows the reaction to proceed halfway, giving rise to nearly half-substituted derivative (**3a**−**3c**), actually as a mixture of regioisomers, having five (in average) saccharide moieties and three unreacted amine functionalities. The maltose, cellobiose, and lactose derivatives are hereafter designated as Mal, Cel, and Lac, respectively, followed by the number 8 (full substitution)[18] or 5 (partial substitution) (Figure 1).

Glycocluster amphiphiles Gly8[18] and Gly5 (Gly = Mal, Cel, or Lac) irreversibly form micellar aggregates, hereafter called glycocluster nanoparticles (GNPs, Scheme 1), in water as already shown for Mal8[16c] and Cel8[17] on the basis of combined evidence from GPC (gel permeation chromatography), DLS (dynamic light scattering), and TEM (transmission electron microscopy).[19] GPC shows that they are aggregated in water, having a pullulan-calibrated molecular weight (mw) of 22400−23500 for Gly8 or 20500−23800 for Gly5, which corresponds to an aggregation number of $n_{agg} = 5$−6 for Gly8 (formular weight, 4172) or 6−7 for Gly5 (3155). DLS indicates that they exclusively form small particles (GNPs) having a size of $d_{DLS} = 4$−5 nm for Gly8 or 5−6 nm for Gly5, which is only slightly larger than the size limit (∼3 nm) of the measurements. The formation of spherical GNPs of that size range is confirmed by TEM (negative staining) for all the members of Gly8 and Gly5 families. The numerical data are summarized in Table 1 and

(19) For a recent review on the aggregation behaviors of glycolipids and related saccharide-functionalized amphiphiles, see: Li, G.; Fudickar, W.; Skupin, M.; Klyszcz, A.; Draeger, C.; Lauer, M.; Fuhrhop, J.-H. *Angew. Chem., Int. Ed.* **2002**, *41*, 1828−1852.
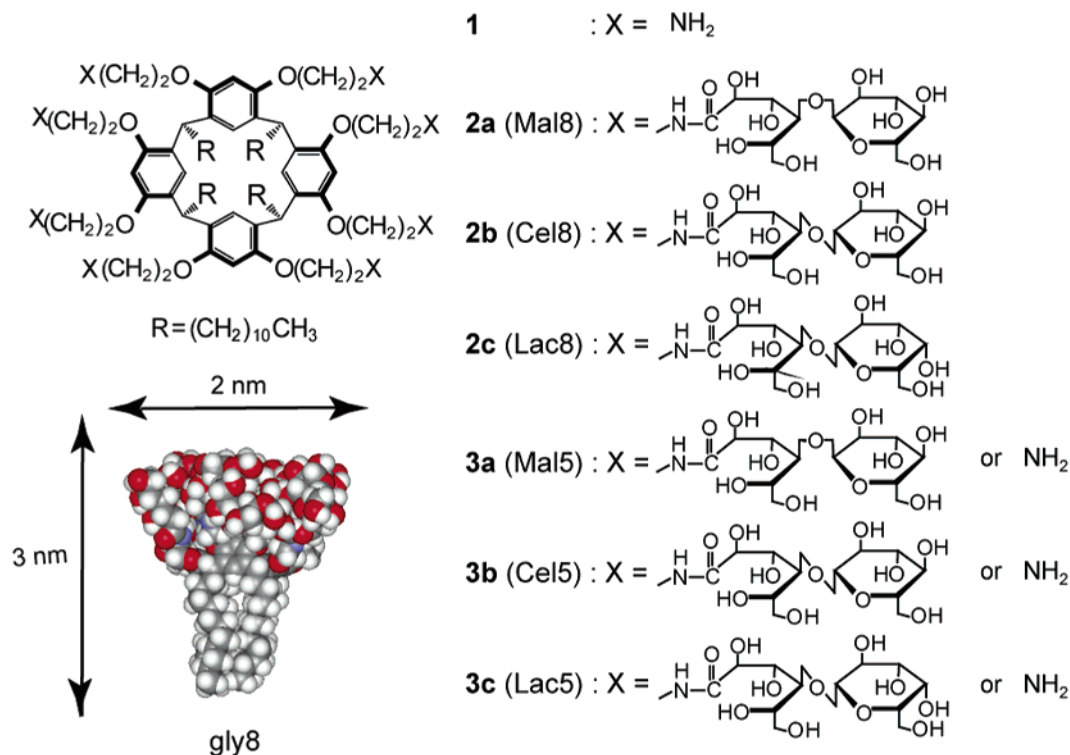
Figure 1. Structure of Gly8 (Mal8, Cel8, and Lac8) and Gly5 (Mal5, Cel5, and Lac5) amphiphiles with a space-filling illustration of Gly8 in the folded conformation.

Scheme 1. Hierarchical Growth of Glycocluster Amphiphile Gly8(5) through GNP to Glycovirus and Its Aggregates
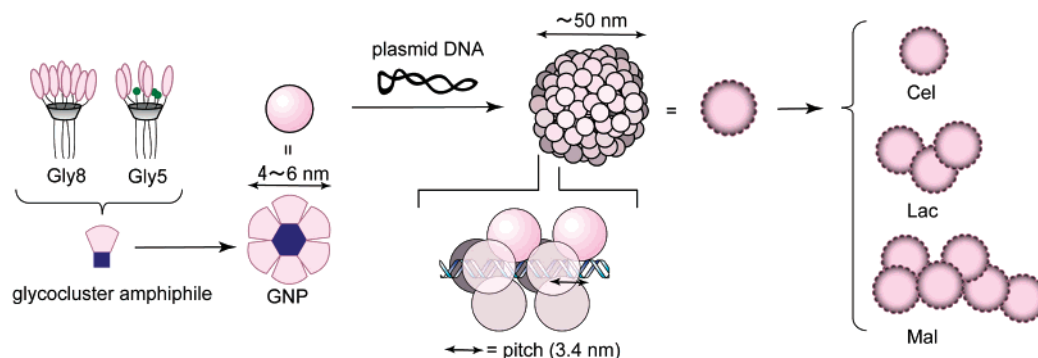

Table 1. Properties of Glycocluster Nanoparticles (GNPs) and Glycoviruses in Water

glycocluster amphiphile Gly8(5)	GNP			glycovirus			
	mw^a	$n_{agg}{}^b$	$d_{DLS}{}^c$ (nm)	$d_{DLS}{}^d$ (nm)	ζ^e (mV)	$E_{Hela}{}^f$ (RLU/mg of protein)	$E_{HepG2}{}^g$ (RLU/mg of protein)
Mal8	22400	5.4	4.2	295	−0.23	3.3×10^3	4.3×10^3
Cel8	23300	5.6	4.7	54	−0.27	8.6×10^6	1.6×10^7
Lac8	23500	5.7	4.7	207	0.09	4.2×10^4	5.2×10^6
Mal5	23500	7.5	5.5	121	−0.22	8.0×10^5	1.4×10^6
Cel5	23800	7.5	5.8	51	−0.12	1.3×10^7	4.2×10^7
Lac5	20500	7.3	5.9	103	−0.05	8.6×10^6	1.2×10^8

^{a} Pullulan-calibrated molecular weight as evaluated by GPC. ^{b} Aggregation number (n_{agg} = mw/fw, where formular weight is fw = 4172 for Gly8 and 3155 for Gly5. ^{c} Mean diameter as evaluated by DLS at [Gly8(5)] = 1.0 mM. ^{d} Mean diameter as evaluated by DLS at [P] = 1.0 μM and Gly8(5)/P = 2.0. ^{e} ζ potential at [P] = 50 μM and Gly8(5)/P = 2.0. ^{f} Transfection efficiency toward Hela cells at Gly8(5)/P = 2.0 with 0.6 μg of pCMVluc. ^{g} Transfection efficiency toward HepG2 cells at Gly8(5)/P = 2.0 with 0.6 μg of pCMVluc.

the actual chromatograms, size profiles, and micrographs are shown in Figures 2 and 3 for representative cases. The size (d_{DLS}) and the aggregation number (n_{agg}) leave little doubt that GNPs arise from "micellization" of the cone-shaped (Figure 1) quadruple-chain/octa(penta)saccharide amphiphiles Gly8(5) (Scheme 1), where the saccharide moieties seem to play

important roles[16c] since there is no evidence for the formation of stable GNP-like particles from octaamine **1** as octaammonium salt **1**·8(HCl).[20]

Glycoviruses and Their Saccharide-Dependent Self-Aggregation. As reported,[17] Cel8-derived GNPs bind to a 7040 bp (base-pair) plasmid pCMVluc having a reporter gene for
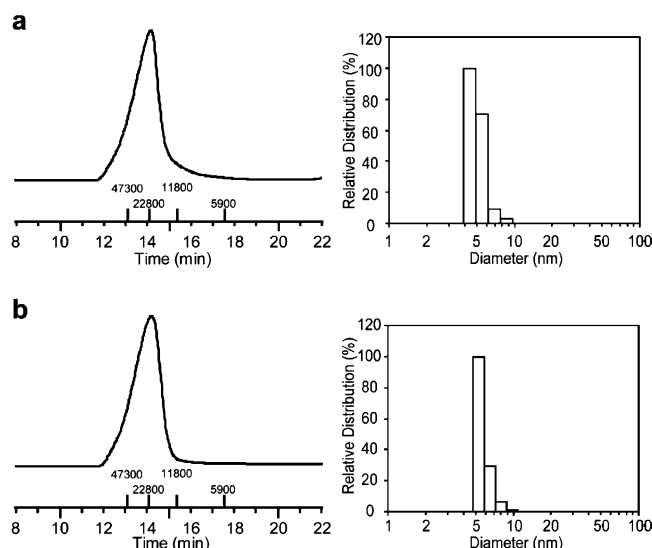
a

b

Figure 2. Gel permeation chromatograms (left) of Lac8 (a) and Cel5 (b) with water as an eluent and size distribution profiles (right) of Lac8 (a) and Cel5 (b) (1 mM) in water in reference to number of particles as evaluated by NICOMP analysis of dynamic light scattering data. The numbers of 5900, 11800, 22800, and 47300 refer to the elution positions of molecular weight markers (pullulans) having respective molecular weights. Those of Mal8, Cel8, Mal5, and Lac5 are essentially the same as shown here.

firefly protein luciferase and a cytomegalovirus promoter to form what we call glycovirus. This is true for any Gly8 or Gly5, although the resulting glycoviral particles undergo saccharide-dependent self-aggregation.

The DNA–Gly8(5) complexation is readily monitored by agarose gel electrophoresis. All the Gly8 and Gly5 members behave similarly in this respect. The DNA is immobilized by Gly8(5) at Gly8(5)/P = 0.2–0.3 (P stands for a base or a phosphate moiety), as typically shown in Figure 4 for Lac8 and Cel5. DLS measurements (Figure 5) reveal that the particle sizes are changeable in the region of Gly8(5)/P = 0.2–0.4 but leveled off upon further increase in Gly8(5)/P. Saturation occurs at Cel8/P ≅ 0.6 (Figure 5b) or Cel5 ≅ 0.8 (5e) and also in a similar range for Mal8(5) and Lac8(5) (Figures 5a, 5c, 5d, and 5f). The saturation sizes (d_{DLS}), however, vary significantly from system to system and are roughly 50 nm for Cel8 and Cel5, 100 nm for Lac5 and Mal5, 200 nm for Lac8, and 300 nm for Mal8.[21] The accurate values at Gly8(5)/P = 2.0, compiled in Table 1, follow the general order of Mal > Lac ≫ Cel and Gly8 > Gly5.

The surface (ζ) potential of the complexes is negative in the presaturation region ($-\zeta = 4-11$ mV at Gly8(5)/P = 0.5) where surface coverage of polyanionic DNA may be incomplete but is rendered neutral after saturation (ζ ≅ 0 mV at Gly8(5)/P = 1.0 or 2.0) (Figure 6 and Table 1) as a result of charge masking by the clustering saccharide moieties.[22]

The TEM images of the complexes taken at Gly8(5)/P = 1.0 (Figure 7) reveal that the variation in size thereof is caused by saccharide-dependent aggregation of the viruses. The micrographs show that (1) unit particles (glycoviruses) of a relatively uniform size (~50 nm) prevail in every case, (2) they are mostly monomeric in case of Cel8 (Figure 7b) and Cel5 (Figure 7e) but are more or less aggregated in other cases (Figures 7a, 7c, 7d, and 7f),[21] (3) the aggregation is more pronounced for Mal8-(5) than for Lac8(5) and for Mal8 and Lac8 than for Mal5 and Lac5, respectively, thus following the same order of Mal > Lac ≫ Cel and Gly8 > Gly5 as in DLS, and (4) the extents of aggregation are in agreement or at least compatible with the saturation DLS sizes of the aggregates (d_{DLS}, Table 1) also shown for each micrograph. The micrographs depend neither on the method of staining (negative (N) or positive (P)) nor on the types of stainers (3% uranyl acetate (Figures 7a–7f, 7i, 7j, and 7l) or 2% sodium phosphotungstate (Figure 7k) for negative staining and 0.6% uranyl acetate (Figure 7g) or RuO₄ (Figure 7h) applied as a vapor for positive staining; compare Figure 7f vs 7g and 7h and 7j vs 7k) and is highly reproducible. Careful inspection of the Mal8, Cel8, and Lac8 viruses in Figures 7i–7l reveals that every particle (glycovirus) is coated with GNPs of a size of 4–6 nm, which is indeed in excellent agreement with that (d_{DLS} = 4–6 nm) of free GNPs (Table 1 and Figure 3). Thus, the saturation is reached upon coverage of DNA with GNPs (Scheme 1). The crucial involvement of GNPs in the interaction with pCMVluc also explains the stoichiometry and size of the unit glycoviral particles, as shown below.

The saturation stoichiometry of Cel8/P ≅ 0.6 and Cel5/P ≅ 0.8 for monomeric Cel8 and Cel5 viruses (Figures 5b and 5e) is equivalent to a saccharide to base-pair ratio of Cel8/bp ≅ 1.2 or Cel5/bp ≅ 1.6 (bp = 2P). Each helical pitch (10 bp) of DNA thus binds ~12 molecules of Cel8 or ~16 molecules of Cel5, which corresponds to ~2 GNPs in reference to the aggregation number (Table 1) of n_{agg} = 5.6 for Cel8-derived GNP or 7.5 for Cel5-derived GNP (12/5.6 ≅ 2 and 16/7.5 ≅ 2). The maximal accommodation of 2 GNPs per pitch is understandable on a steric ground. The present GNP–DNA complexation, which may bear a relevance to the nucleic acid binding with glycoside antibiotics[23] and polysaccharides,[24] must be driven by multiple hydrogen-bonding between the OH groups of GNPs and the phosphate groups of DNA.[16,17] Such an interaction would be maximized when GNPs (d ≅ 4 nm for DNA-bound GNPs, Figures 7j and 7k) are aligned along the major groove (1.3 nm width and 3.4 nm pitch length) of DNA. Models indicate that 2 GNPs could be accommodated in a pitch

(20) Octaammonium salt **1**·8(HCl) readily binds to pCMVluc to form electrophoretically immobile complex(es) even at a stoichiometric ratio, i.e., **1**·8(HCl)/P ≅ 0.15 or N/P ≅ 1. DLS shows a multicomponent size distribution profile, composed of relatively large particles with approximate size of 100 and 600 nm in addition to smaller ones (~30 nm). Surface plasmon resonance (SPR) indicates that pCMVluc is rapidly adsorbed on and desorbed from monolayer **1**·8(HCl) assembled on a hydrophobized sensor chip of SPR. All the observations suggest that the **1**·8(HCl)–pCMVluc complexation is promoted by electrostatic forces possibly with hydrophobic assistance and is different in nature from the practically irreversible Gly8-(5)–pCMVluc complexation driven by multiple hydrogen-bonding between polyphosphate chain of DNA and sugar OH groups of GNPs. Complex **1**·8(HCl)–pCMVluc is transfection active. In marked contrast to Gly8-(5)–pCMVluc complexes, however, it is highly cytotoxic, the cell viability being ~20% at **1**·8(HCl)/P ≥ 1.0 under the present transfection conditions.

(21) The sizes of glycoviral particles are rough multiples of that of the monomeric unit particle (~50 nm); d_{DLS} ≅ 50n, where n = 1 for Cel8 and Cel5, 2 for Lac5 and Mal5, 4 for Lac8, and 6 for Mal8. The upper limits of aggregation numbers for Mal and Lac viral particles in case of closest spherical packing are given by 0.76V/v = 0.76n^3, where V and v represent the volumes of spheres with a diameter of 50n nm or 50 nm, respectively. The micrographs (Figure 7) suggest that they are not so closely packed as this index suggests. The actual aggregation numbers would be 2–3 for Cel5 and Lac5, around 10^1 for Lac8, and somewhere between 10^1 and 10^2 for Mal8.

(22) The amine/phosphate ratio in complex Gly5–pCMVluc at saturation (Gly5/P ≅ 0.8) is N/P ≅ 2.4, i.e., in amine excess. The ammonium charge if any may also be shielded by the saccharide clusters. For similar charge-masking effects of appended saccharides, see: (a) ref 6t. (b) Erbacher, P.; Bettinger, T.; Belguise-Valladier, P.; Zou, S.; Coll, J.-L.; Behr, J.-P.; Remy, J.-S. *J. Gene Med.* **1999**, *1*, 210–222.

(23) (a) Fourmy, D.; Recht, M. I.; Blanchard, S. C.; Puglisi, J. D. *Science* **1996**, *274*, 1376–1371. (b) Sucheck, S. J.; Wong, C.-H. *Curr. Opin. Chem. Biol.* **2000**, *4*, 678–686.

(24) (a) Sakurai, K.; Shinkai, S. *J. Am. Chem. Soc.* **2000**, *122*, 4520–4521. (b) Sakurai, K.; Mizu, M.; Shinkai, S. *Biomacromolecules* **2001**, *2*, 641–650.
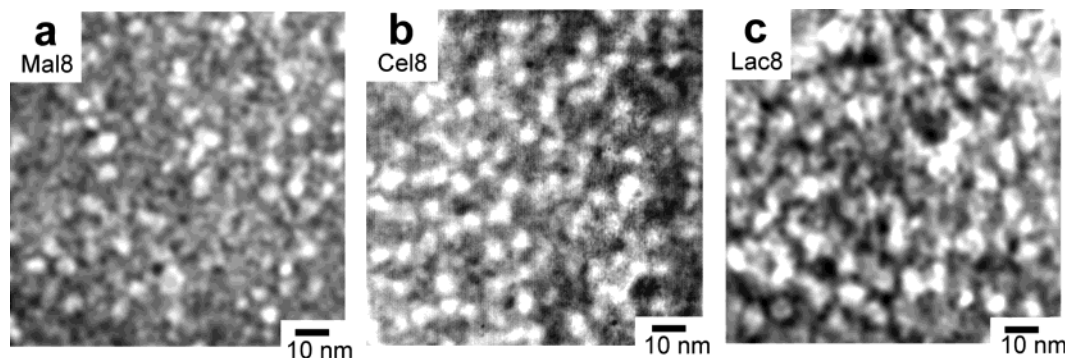
Figure 3. Transmission electron microscopic (TEM) images of GNPs observed for a solution of Mal8 (a), Cel8 (b), and Lac8 (c) (1 mM) in water with uranyl acetate (2 wt %) as a negative stainer. Mal5, Cel5, and Lac5 give similar images.
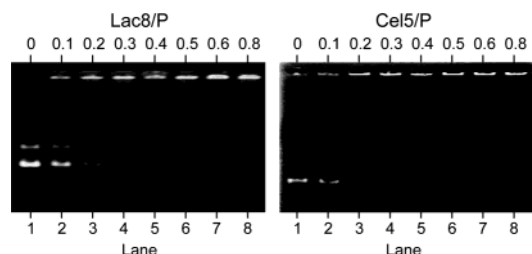

Figure 4. Electrophoretic gel shifts for pCMVluc in the absence (lane 1) and presence of increasing amounts (lanes 2−8) of Lac8 (a) and Cel5 (b), using 0.7% agarose gel in 40 mM Tris-acetate buffer. Similar shift patterns are observed for Mal8, Cel8, Mal5, and Lac5.

without steric interference when located at north and south or east and west pitch by pitch (Scheme 1).

The saturation stoichiometry of 2 GNPs per pitch (10 bp) also defines the composition of the present glycoviral complex encapsulating 7040 bp plasmid pCMVluc as pCMVluc·(∼1400)-GNP ($2 \times 7040/10 \cong 1400$). The volume of pCMVluc, assuming a cylinder with a cross-sectional diameter of 2 nm, is $V_{DNA} = \pi(2/2)^2 \times 3.4 \times (7040/10) \cong 7500$ nm^3. That of 1400 spherical ($d = 4$ nm) GNPs with a void volume of 26% at closest packing would be $V_{GNP} = 1400 \times 4\pi/3 \times (4/2)^3/0.74 \cong 63000$ nm^3. The sum of these, that is, $V_{DNA} + V_{GNP} = 70500$ nm^3, represents the lower limit of the volume of the complex and is very close to the real volume of the monomeric Cel8 and Cel5 viruses (Figures 7b and 7e) and unit particles of other Mal8(5) and Lac8(5) systems (Figures 7a, 7c, 7d, and 7f), all having a size of $d \cong 50$ nm ($V_{virus} = 4\pi/3 \times (50/2)^3 = 65000$ nm^3, assuming a sphere). There is no doubt, in reference to the criteria of artificial viruses (Introduction), that the present unit glycoviral complex contains a single molecule of DNA as a template, exhibits a definable stoichiometry of 2 GNPs per helical pitch, and is highly efficiently packed in a viral size (Scheme 1), resulting in dense GNP-coating of the surface (Figures 7i−7l) and effective charge shielding ($\zeta \cong 0$ mV). It is remarkable that the otherwise nonadhesive GNPs when free are closely packed when aligned on the DNA template.

It is in self-aggregation that the present glycoviruses manifest their saccharide specificities. As far as micrographs (Figure 7) are concerned, the glycoviral aggregation is more appropriately viewed as adhesion rather than fusion and may involve inter-viral saccharide−saccharide interactions. This itself is not surprising, since cell-surface oligosaccharides are responsible for various adhesion processes,[25,26] some of which are even believed to be triggered by direct saccharide−saccharide

interactions.[27] At the same time, it may not be unreasonable to expect that the present glycoviruses would be free from aggregation in view of the highly hydrophilic nature of the glycoclusters.[16c] What is really remarkable is the big difference in the aggregation tendencies of otherwise closely related Mal, Cel, and Lac viruses. Both DLS (Figure 5) and TEM (Figure 7) results using different samples are highly reproducible and confirm that Cel viruses are mostly monomeric, Mal viruses are highly aggregated, and Lac viruses exhibit an intermediate oligomeric behavior (Scheme 1). This is true for both Gly8 and Gly5 and aggregation is more pronounced for the Gly8 viruses than Gly5, suggesting that the amine/ammonium functions definitely involved in Gly5 have no essential roles here. Thus, the differing aggregation/adhesion tendencies in the order Mal > Lac ≫ Cel must reflect a subtle difference in the terminal saccharide moieties, i.e., α-glucoside in Mal, β-galactoside in Lac, and β-glucoside in Cel. While we have no good explanation here, the present results indicate that an alteration in stereo-chemistry of a single glycoside linkage (Mal vs Cel) or a single OH group on a pyranose ring (Cel vs Lac) can result in drastic change in the adhesion properties of glycoclusters.

Transfection. The preliminary study indicates[17] that Cel8 virus transfects Hela cells in a serum-free medium and more

(25) (a) Eggens, I.; Fenderson, B.; Toyokuni, T.; Dean, B.; Stroud, M.; Hakomori, S. *J. Biol. Chem.* **1989**, *264*, 9476−9484. (b) Rojo, J.; Morales, J. C.; Penadés, S. *Top. Curr. Chem.* **2002**, *218*, 45−92. (c) References 24h,l,m. (d) Santacroce, P. V.; Basu, A. *Angew. Chem., Int. Ed.* **2003**, *42*, 95−98.

(26) (a) Lee, Y. C.; Lee, R. T. *Acc. Chem. Res.* **1995**, *28*, 321−327. (b) Hakomori, S. *Glycoconjugate J.* **2000**, *17*, 627−647. (c) Bertozzi, C. R.; Kiessling, L. L. *Science* **2001**, *291*, 2357−2364. (d) Roth, J. *Chem. Rev.* **2002**, *102*, 285−304. (e) Ritchie, G. E.; Moffat, B. E.; Sim, R. B.; Morgan, B. P.; Dwek, R. A.; Rudd, P. M. *Chem. Rev.* **2002**, *102*, 305−320. (f) Zachara, N. E.; Hart, G. W. *Chem. Rev.* **2002**, *102*, 431−438.

(27) For recent studies on synthetic multivalent saccharide clusters, see: (a) Lee, W. J.; Spaltenstein, A.; Kingery-Wood, J. E.; Whitesides, G. M. *J. Med. Chem.* **1994**, *37*, 3419−3433. (b) Choi, S. K.; Mammen, N.; Whitesides, G. M. *J. Am. Chem. Soc.*, **1997**, *119*, 4103−4111. (c) Zanini, D.; Roy, R. *J. Org. Chem.* **1998**, *63*, 3486-3491. (d) Matsuura, K.; Tsuchida, A.; Okahata, Y.; Akaike, T.; Kobayashi, K. *Bull. Chem. Soc. Jpn.* **1998**, *71*, 2973−2977. (e) Pavlov, G. M.; Korneeva, E. V.; Jumel, K.; Harding, S. E.; Meijer, E. W.; Peerlings, H. W. I.; Stoddart, J. F.; Nepogodiev, S. A. *Carbohydr. Polym.* **1999**, *38*, 195−202. (f) Gordon, E. J.; Gestwicki, J. E.; Strong, L. E.; Kiessling, L. L. *Chem. Biol.* **2000**, *7*, 9−16. (g) Fulton, D. A.; Stoddart, J. F. *Org. Lett.* **2000**, *2*, 1113−1116. (h) Matsuura, K.; Kitakouji, H.; Sawasa, N.; Ishida, H.; Kiso, M.; Kitajima, K.; Kobayashi, K. *J. Am. Chem. Soc.* **2000**, *122*, 7406−7407. (i) Matsuura, K.; Hibino, M.; Yamada, Y.; Kobayashi, K. *J. Am. Chem. Soc.* **2001**, *123*, 357−358. (j) de la Fuente, Barrientos, A. G.; Rojas, T. C.; Rojo, J.; Canãda, J.; Fernández, A.; Penadés, S.; *Angew. Chem., Int. Ed.* **2001**, *40*, 2258−2261. (k) Tromas, C.; Rojo, J.; de la Fuente, Barrientos, A. G.; García, R.; Penadés, S. *Angew. Chem., Int. Ed.* **2001**, *40*, 3052−3055. (l) Haseley, S. R.; Vermeer, H. J.; Kamerling, J. P.; Vliegenthart, J. F. G. *Proc. Natl. Acad. Sci. U.S.A.* **2001**, *96*, 9419−9424. (m) Hernáiz, M. J.; de la Fuente, J. M.; Barrientos, Á. G.; Penadés, S. *Angew. Chem., Int. Ed.* **2002**, *41*, 1554−1557. (n) Gestwicki, J. E.; Cairon C. W.; Strong, L. E.; Oeyjen, K. A.; Kiessling, L. L. *J. Am. Chem. Soc.*, **2002**, *124*, 14922−14933.
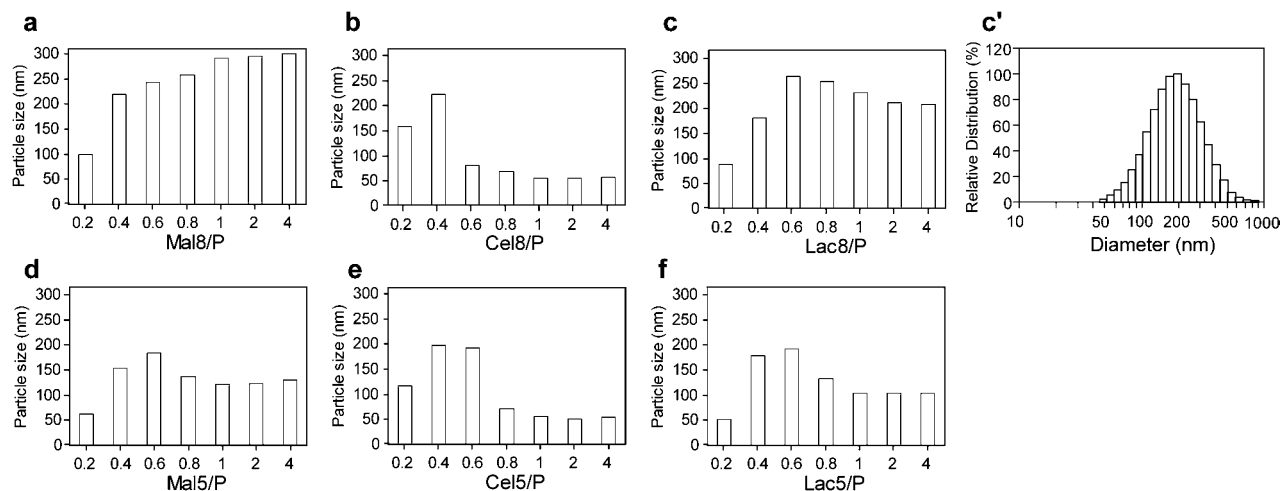
Figure 5. Variation in the mean DLS sizes of Gly8(5)−pCMVluc complexes (Gly = Mal, Cel, or Lac) arising from pCMVluc (1 μM P) in the presence of increasing amounts of Gly8(5) in HEPES buffer (10 mM, pH 7.4, [NaCl] = 150 mM) in water in reference to number of particles as evaluated by Gaussian analysis of dynamic light scattering data. The size distribution profile for Lac8−pCMVluc complex at Lac8/P = 2.0 with an average size of ~200 nm is shown in panel c′.
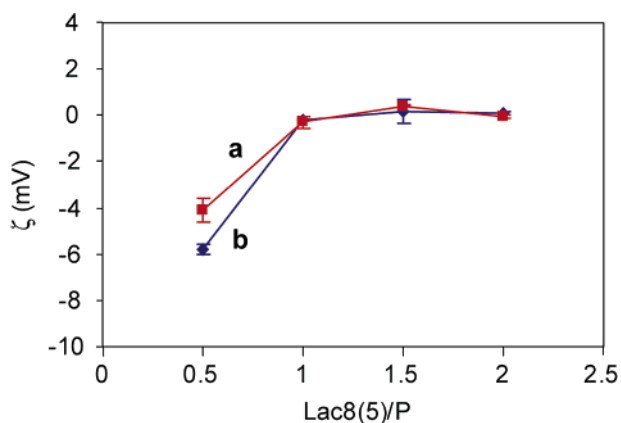

Figure 6. ζ potentials (for triplicate measurements) of Lac8-pCMVluc (a) and Lac5-pCMVluc (b) complexes (50 μM P) at Lac8(5)/P = 0.5, 1.0, 1.5, or 2.0 in HEPES buffer (10 mM, pH 7.4, [NaCl] = 150 mM). Similar potential−Gly8(5)/P profiles are observed for Mal8 and Mal5 as well as for Cel8 and Cel5.

efficiently (by a factor of 50−100%) in the presence of fetal bovine serum (10%) with little cytotoxicity, with the serum-free transfection efficiency being approximately 1 order of magnitude higher than that of lipofectin, a standard cationic vector. Here we consider hepatic (liver) cells HepG2 in addition to Hela cells as a reference. The transfection efficiencies (E), expressed in terms of relative light units (RLU) for chemiluminescent luciferase formed in the cells, are essentially constant in the saturation range (Gly8(5)/P = 1.0−4.0) at a fixed amount of DNA (0.6 μg per run) and exhibit a saturation behavior with increasing amounts of DNA at fixed Gly8(5)/P = 2.0, as shown for Lac5 virus with HepG2 cells in Figure 8.

The variation in the activities of different viruses at Gly8-(5)/P = 2.0 is remarkable.[20] With Hela cells, they range from 1.3×10^7 for Cel5 to 3.3×10^3 for Mal8 with a span of Cel5/Mal8 = 4×10^3 at Gly8(5)/P = 2.0. The activities are size-regulated; plots of log E vs d_{DLS} give an excellent linear correlation with a negative slope of -0.0153 Δ(log E)/nm (Figure 9a). In Figure 9b is shown a similar log E vs size correlation for hepatic HepG2 cells which possess specific receptors for asialoglycoproteins[28] whose terminal β-galactose

residues are responsible for binding to the receptors. Two factors operate here. One is a nonspecific size factor. The transfection by Cel8, Cel5, Mal8, and Mal5 viruses having receptor-inert glucose residues is size-controlled in a quite similar manner as above for Hela cells; there is no notable cell selectivity (E_{HepG2}/E_{Hela} = 1.3−3.3) and the size sensitivities, i.e., the slopes of the semilogarithmic linear size−activity correlations, are almost the same for two types of cells. The other is a receptor factor. The Lac8 and Lac5 viruses having galactose moieties as ligands of the receptors are significantly HepG2-selective (E_{HepG2}/E_{Hela} = 120 for Lac8 and 14 for Lac5) and their activities therefor are higher by a factor of ~10^2 than expected on the size basis. This advantage of Lac8 and Lac5 toward hepatic cells (red bars in Figure 9b) is almost completely (>98%) lost when asialofetuin (AF), a typical asiologlycoprotein which is firmly bound to the receptors, is added as an inhibitor; the efficiencies of inhibited transfection (shown with a mark +AF in Figure 9b) nicely fall on the size−activity line. In marked contrast, AF essentially has no effect on Cel8, Mal8, or Mal5 (Figure 9b). The specific preference (red bars) of galactose-functionalized Lac8 and Lac5 viruses for the receptor-containing HepG2 cells can be unambiguously ascribed to the receptor-mediated pathway.

Endocytosis and Size Effect Therein. The cells continually ingest a part of their plasma membrane via endocytosis to form endocytic vesicles.[14] Solvent and solute can be taken up into the cells by the endocytosis activity of the latter. Gene delivery usually takes advantage of this endocytic pathway.[3] Endocytic vesicles incorporating DNA-bearing particles are transferred to endosomes and then to lysosomes, where liberation of DNA somehow takes place. The generally accepted role of conventional amine/ammonium vectors, in addition to that of DNA binders, is 2-fold. As ammonium cations, they bind to negatively charged cell surfaces to trigger endocytosis. As free-base amines, they serve as "proton sponges" and promote lysosomal membrane disruption to liberate the DNA.[13f] The present glycoviral vectors with $\zeta \cong 0$ mV, particularly the fully substituted Gly8 vectors, possess none of these amine/ammonium advantages. While a detailed mechanism of the present gene delivery system

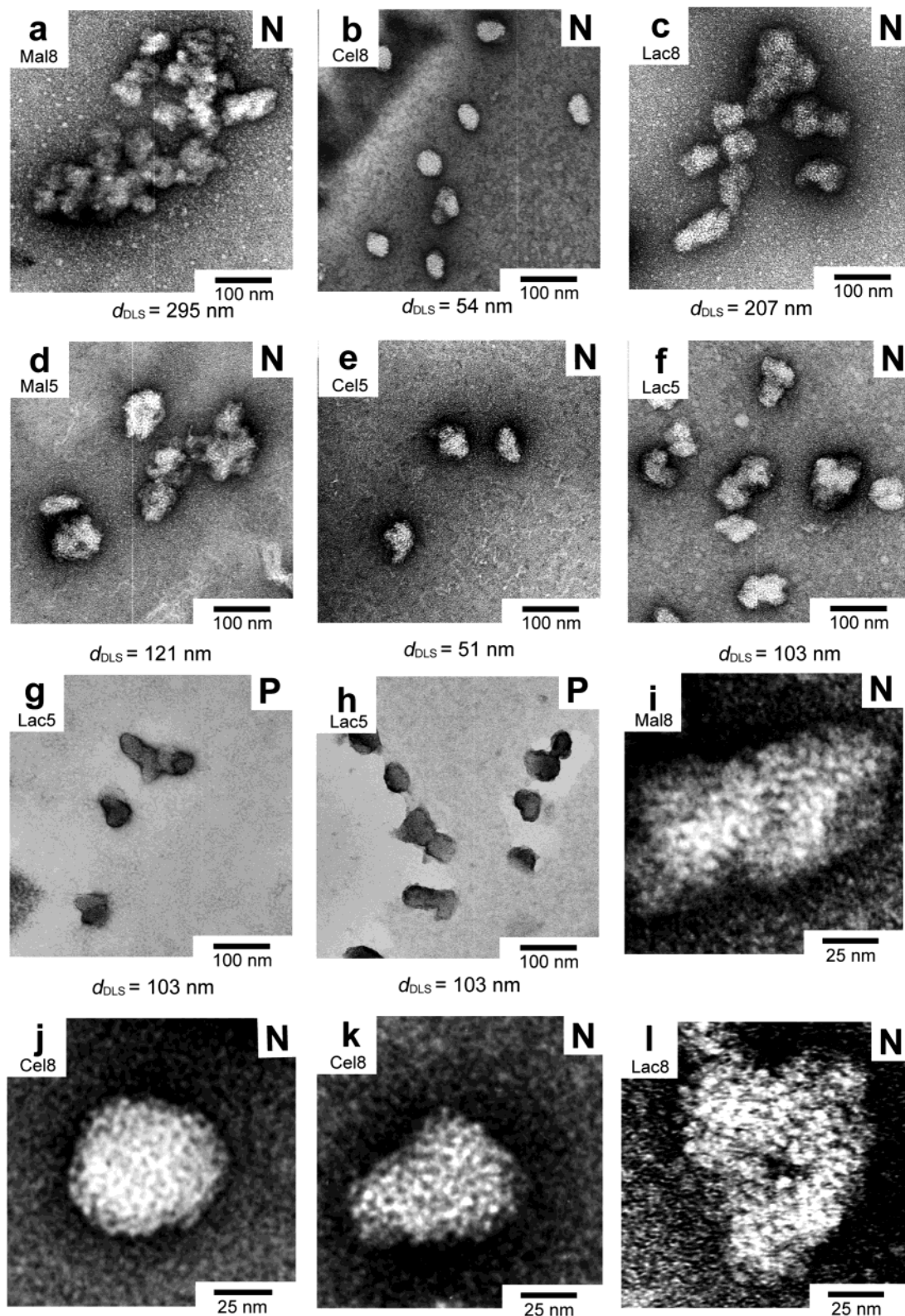(28) Ashwell, G.; Hanford, J. *Annu. Rev. Biochem.* **1982**, *51*, 531−554.

Figure 7. Transmission electron microscopic (TEM) images of Gly8(5)−pCMVluc complexes (glycoviruses) as observed for a solution of pCMVluc (50 μM P) and at Gly8(5)/P = 1.0 in water (a−h). N and P stand for negative staining with uranyl acetate (3 wt %) as a negative stainer (a−f, i, j, and l) and positive staining with uranyl acetate (0.6%) (g) or RuO$_4$ (vapor) (h) as a positive stainer, respectively. d_{DLS} is mean diameter of the complex as evaluated by DLS at [P] = 1.0 μM and Gly(5)/P = 2.0 (cf. Table 1). Panels i−l: enlargement of glycoviral particle with uranyl acetate (3 wt %) (i, j, l) or sodium phosphotungstate (2%) (k) as a negative stainer.

remains to be uncovered, it is readily shown, based on direct and indirect evidence, that it follows the general endocytic pathway.

Indirect evidence comes from inhibition studies. The endocytic activity is known to be lost at 4 °C[29] and is inhibited by a number of drugs including cytochalasin B[30] and wortman-
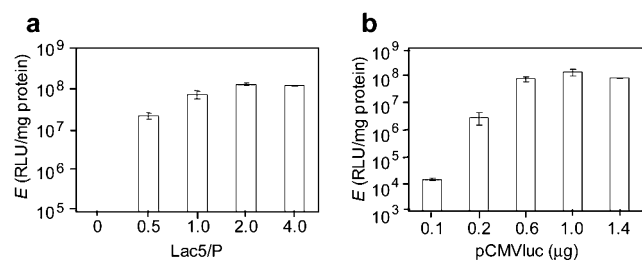
Figure 8. Lac5-mediated transfection of Hela cells. Luciferase expression efficiencies (E, for triplicate measurements) in terms of chemiluminescence relative light units (RLU) per mg of total protein in the cells ($<10^4$ at Lac5/P $= 0$) as a function of Lac5/P with a fixed amount (0.6 μg per run) of pCMVluc (4.5 μM P) (a) or as a function of amount of pCMVluc at fixed Lac5/P = 2.0 (b).
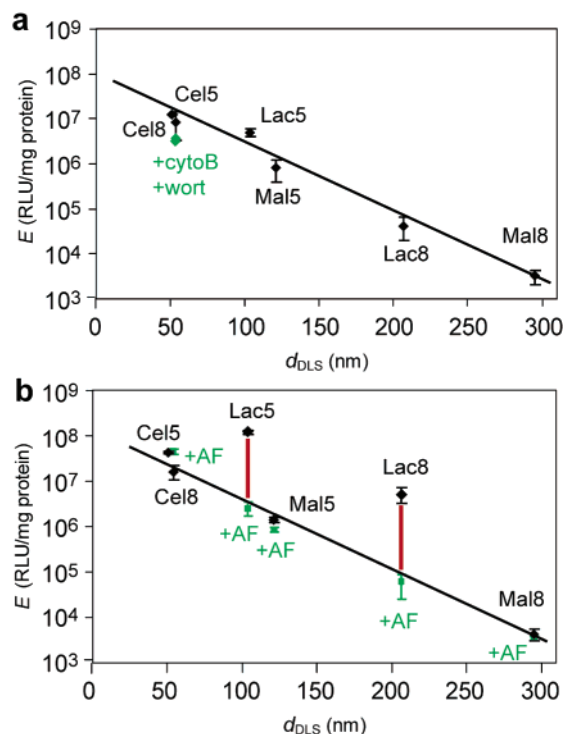

Figure 9. Gly8(5)-mediated transfection of Hela cells (a) and HepG2 cells (b) with a fixed amount (0.6 μg per run) of pCMVluc (4.5 μM P) at Gly8-(5)/P = 2.0. Luciferase expression efficiencies (E, for triplicate measurements) in terms of chemiluminescence relative light units (RLU) per mg of total protein in the cells ($<10^4$ at Gly8(5)/P $= 0$) as a function of mean DLS sizes of the glycoviral particles at Gly8(5)/P =2.0. Those with a mark +AF, +cytoB, or +wort refer to the runs in the presence of asialofetuin (0.5 mg/mL), cytochalasin B (50 μM), or wortmannin (10 μM), respectively.

nin.[31] This is the case here. The Cel8-mediated transfection of Hela cells is ∼60% inhibited by these inhibitors (Figure 9a) at [cytochalasin B] = 50 μM or [wortmannin] = 10 μM and does not take place at all at 4 °C. Fluorescence labeling, on the other hand, provides direct evidence.[29] Endosomes and plasmid DNA (pCMVluc) can be labeled with green-fluorescing GFP (green fluorescent protein) and red-fluorescing tetramethylrhodamine, respectively. The modified plasmid behaves (electrophoresis) similarly as the unmodified one and binds to Cel8 to give viral

(29) Wickham, T. J.; Mathias, P.; Cheresh, D. A.; Nemerow, G. R. *Cell* **1993**, *73*, 309−319.
(30) Brisson, M.; Tseng, W. C.; Almonte, C.; Watkins, S.; Huang, L. *Hum. Gene Ther.* **1999**, *10*, 2601−13.
(31) Martys, J. L.; Wjasow, C.; Gangi, D. M.; Kielian, M. C.; McGraw, T. M.; Backer, J. M. *J. Biol. Chem.* **1996**, *271*, 10953−10962.

particles with $d_{DLS} = 53$ nm at Cel8/P $= 1.0$. The uptake of plasmid-labeled viruses by endosome-labeled Hela cells can be monitored by fluorescence microscopy (Figure 10) after incubation at either 37 or 4 °C, followed by thorough washing of the cells. Green-labeled endosomes manifest themselves upon excitation at 470−490 nm (a). Red-labeled plasmid finds itself, upon excitation at 520−550 nm, in the cells incubated at 37 °C but not at 4 °C (b). Computer overlap of the two micrographs, i.e., red plasmid and green endosomes, affords merged yellow-to-orange spots (c). This confirms that the plasmid is indeed incorporated in the endosomes and hence must have been taken into the cells via endocytosis which is effective at 37 °C but not at 4 °C.

The size dependence of the transfection efficiencies shown in Figure 9a is understandable in terms of endocytosis. This size−activity correlation cannot necessarily be interpreted literally as such, since it is also explainable in terms of varying fractions of particular transfection-active species. The particular form of endocytosis carried out by essentially all eukaryotic cells is pinocytosis (cellular drinking), which takes up guest objects in pinocytic vesicles of a size of ∼100 nm.[14] If this is true for the present system, only monomeric viruses ($d \cong 50$ nm) could be accommodated. The present glycoviral aggregates are polydispersed as shown by the microscopic appearance (Figure 7) as well as by the actual size distribution profile for the Lac8 virus at Lac8/P $= 2.0$ (Figure 5c′). The polydispersion may reflect the reversible nature of the aggregation, giving rise to an equilibrium mixture of monomer, dimer, trimer, and so on.[21] With increasing inter-viral interactions, the most populated one would be shifted toward higher oligomers with increasing mean DLS sizes (d_{DLS}). If only monomer (monomeric virus) is transfection-active, the transfection efficiencies would be governed by the fraction thereof, which decreases with increasing d_{DLS}. We prefer this interpretation for the size effect (Figure 9a), although we need to get a deeper insight into the implication of semilogarithmic linear size−activity correlation. Whatever the mechanistic details may be, it is doubtless that monomeric viruses are far more active than their aggregates.

The size effects in cationic gene delivery have been studied rather extensively.[13] A generally accepted view is that smaller particles are preferred. The size limit of <100 nm for the accommodation in endocytic vesicles has also been suggested.[13a] Nevertheless, it is not easy to extract the pure size effects in the presence of concurrent charge effects. Indeed, essentially in all the cases, efficient transfection requires a net cation excess. Cationic amine−DNA complexes are readily adsorbed on negatively charged cell surfaces and may invade the cells via "enforced" endocytosis or other mechanism. Such an electrostatic contribution would be more pronounced for bigger complexes having larger surface areas and may compensate the intrinsic size effect of endocytosis, favoring smaller complexes. With this being the case, the overall transfection efficiencies may be rendered less size-sensitive. This is probably the current situation of cationic in vitro gene delivery, where μm-sized large particles can be used,[11] sometimes even more effectively.[32] The present glycoviruses having minimized electrostatic/hydrophobic contributions provide an ideal set of size markers. The results in Figure 9a not only reinforce the above concepts but also

(32) Ogris, M.; Steinlein, P.; Kursa, M.; Mechtler, K.; Kircheis, P.; Wagner, E. *Gene Ther.* **1998**, *5*, 1425−1433.
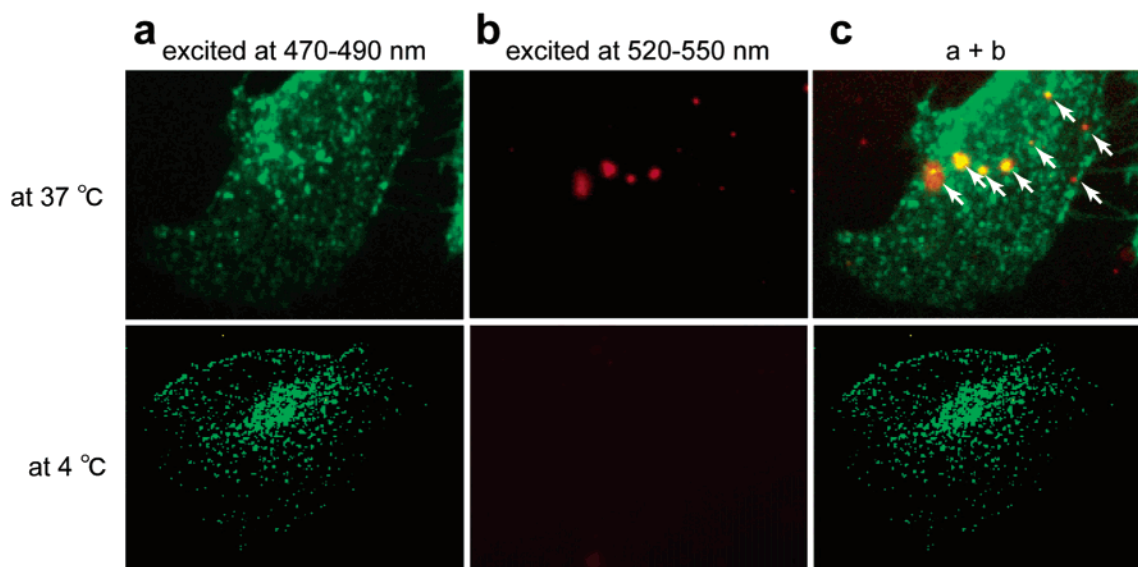
Figure 10. Fluorescence micrographs of GFP-labeled (for endosomes) Hela cells treated with tetramethylrhodamine-labeled (for plasmid pCMVluc) Cel8 virus at Cel8/P = 1.0 in Opti-MEM at either 37 or 4 °C for 30 min, followed by washing of the cells. (a) Excitation at 470−490 nm, showing labeled endosomes. (b) Excitation at 520−550 nm, showing labeled plasmid. (c) Computer overlap of a and b. Arrows indicate yellow-to-orange spots arising from merge of green and red colors.

establish the charge-free size effects in glycoviral gene delivery, where only monomeric viruses undergo effective size-allowed endocytosis (pinocytosis).

Receptor-Mediated Gene Targeting Still under Size Control. The transfection of hepatic HepG2 cells is dually controlled by the specific receptor factor and the nonspecific size factor. In other words, the specific receptor pathway is still under strict size control. In the context of the preceding discussion, only monomeric viruses (∼50 nm) would be allowed to have facilitated access to the asialoglycoprotein (ASGP) receptors. Ligand size has been the subject of a number of investigations.[33] There is good evidence that the upper limit for uptake and processing of ligands by the ASGP receptor is ∼90 nm.[34] This nicely agrees with the present results. Relative contributions of the two factors are also noteworthy. That of receptor-mediated pathway activates the otherwise inactive Lac8 and Lac5 viruses by a factor of ∼10^2 (red bars in Figure 9b). In magnitude, this specific activation corresponds to a nonspecific size reduction by 130 nm ((-0.0153) × (-130) = 2, where -0.0153 is the slope of semilogarithmic size−activity correlation in Figure 9b). Thus, the receptor factor is neither overwhelming the size factor nor overwhelmed thereby. Apparent confusion easily arises. While the transfection of HepG2 by Lac8 and Lac5 viruses is almost completely (>98%) receptor-mediated, their activities are only comparable to those of receptor-inert Cel8 and Cel5 viruses. This is because the Lac viruses are mostly oligomeric and the Cel viruses monomeric, resulting in compensation of size/receptor advantage/disadvantage. The difference between Lac8 and Lac5 is also due to their different sizes.

There has been an intense recent concern about gene targeting to hepatic cells by using cationic vectors partially functionalized

with galactose moieties.[6] The apparent effects of such a galactose modification are slight to moderate (E_{mod}/E_{unmod} = 10^1−10^2)[6n] in many cases and can be even inhibitory (E_{mod}/E_{unmod} < 1) in some cases, where the index E_{mod}/E_{unmod} refers to the ratio of modified vs unmodified transfection efficiencies for hepatic cells. It is also dependent on N/P or vector/DNA ratios and changes in a range of 10^{-1}−10^5 with varying N/P in a particular polyethyleneimine case.[6n] The present results suggest that index E_{mod}/E_{unmod} is not a good measure of receptor contribution, since galactose modification can change the size as well (Lac5 < Lac8).[20] Such a size-altering effect of galactose modification may be calibrated by using a glucose-modified vector as a reference. In this respect too, one has to be extremely careful, since, at least in the present system, β-glucose (Cel8 and Cel5) and α-glucose (Mal8 and Mal5) behave drastically differently as regards the size effects. Depending on which of Mal and Cel is taken as a reference, the galactose/glucose selectivities in the transfection of hepatic HepG2 cells vary dramatically; Lac8/Mal8 = 1200, Lac5/Mal5 = 87, Lac5/Cel5 = 2.9, and Lac8/Cel8 = 0.32 (Figure 9b and Table 1).

Concluding Remarks

A hidden key word of this work is charge. Clearly, the amine/ammonium characteristic functions are by no means the prerequisites of artificial vectors. In the absence of charge effects is revealed a quantitative size correlation in neutral glycoviral gene delivery; this in turn allows the receptor route to be well characterized. A brief summary follows. (1) Glycoviruses arising from size-controlled gene coating with glycocluster nanoparticles (GNPs) undergo saccharide-dependent (Mal > Lac ≫ Cel or α-Glc > β-Gal ≫ β-Glc) self-aggregation. (2) Cells (Hela and HepG2) are transfected by these viruses via a nonspecific but highly size-regulated endocytic pathway, where only monomeric viruses possess substantial transfection activities. The intrinsic function of viruses, that is, cell invasion followed by gene expression, seems to be also intrinsic to size-manipulated (monomeric) artificial viruses. (3) The transfection of HepG2 cells by the galactose-functionalized Lac viruses which happen

(33) (a) Schlepper-Schäfer; Hulsman, J.; Djovkar, A.; Meyer H. E.; Herbertz, L.; Kolb, H.; Kolb Bachofen, V. *Exp. Cell Res.* **1986**, *165*, 494−506. (b) Bijsterbosch, M. K.; Ziere, G. L.; van Berkel, T. J. *Mol. Pharmacol.* **1989**, *36*, 484−489. (c) Bijsterbosch, M. K.; Ziere, G. L.; van Berkel, T. J. *Biochem. J.* **1990**, *270*, 233−239. (d) Ferkol, T.; Perales, J. C.; Mularo, F.; Hanson, R. W. *Proc. Natl. Acad. Sci. U.S.A.* **1996**, *93*, 101−105.

(34) Rensen, P. C.; Sliedregt, L. A.; Ferns, M.; Kieveit, E.; van Rossenberg, S. M.; van Leeuwen, S. H.; van Berkel, T. J.; Biessen, E. A. *J. Biol. Chem.* **2001**, *276*, 37577−37584.

to be oligomeric is receptor-mediated but size-depressed; the otherwise sizable receptor advantage ($\sim 10^2$) is mostly canceled by the size factor. (4) The size effects thus deeply penetrate into the transfection activities. One has to be careful when comparing different vectors even in reference to apparently slight modification.

There are a number of future concerns. From a mechanistic viewpoint, what remains to be uncovered is the fate of glycoviruses especially in reference to how the virus escapes from endosomes/lysosomes and how the plasmid is released from the virus. As regards efficient hepatocyte targeting, the galactose-cluster motifs have to be manipulated to meet the two requirements of maximal virus−receptor interaction and minimal viral aggregation. Self-replicating glycoviruses may also be an intriguing future target.

In relevance to biological hierarchy, the growth of glyco-cluster amphiphile Gly8(5) through GNP to transfectious glycovirus represents a bionanotechnological bottom-up construction of functional nanometric sizes for which pharmacological and immunological applications are also conceivable.[35] Number-, size-, and shape-control are common in biological macromolecular associations with viruses, ribosomes, fibrils, protein subunit structures, etc. as examples but difficult to achieve in artificial systems. Abiological interactions have so far been mostly concerned with small convergent systems of the host−guest type or infinite divergent systems such as crystals, gels, and surfaces, although number- and size-control in supramolecular oligomerization,[36] finite macromolecular association,[37] topologically programmed multimolecular metal coordination,[38] and hierarchical self-assembly[39] are rapidly growing areas. An unanswered question here in regard to the shape- and size-control is why the DNA−GNP complex pCMVluc·($\sim$1400)GNP is closely and spherically packed even when free GNPs are not aggregating.[40] The simplest answer

would be to assume a general entropic preference of intraparticle processes, intraviral inter-GNP saccharide−saccharide interactions in the present case. In this context, intraparticle inter-saccharide interactions may be efficient enough to keep the integrity of GNP and the spherically packed structure of the virus, while inter-GNP interactions would not be so effective as to induce aggregation thereof; inter-viral aggregation, on the other hand, is saccharide-dependent. Such a remarkable adhesion control of multivalent saccharide clusters may have relevance to the roles of cell-surface oligosaccharides.[23−25] For better performance of artificial glycoviruses and related nanoparticles, their aggregation is an annoying problem and should be avoided. We need to get a deeper insight into what the driving force of aggregation is and how it is affected by the nature (identity and stereochemistry) of saccharides involved. Definitely, we will have to face the most puzzling question raised by the present work; why is α-glucose highly aggregating while β-glucose not al all?

JA035636F

(35) For applications of synthetic receptors to protein surface recognition, see for example: (a) Hamuro, Y.; Calama, M. C.; Park, H. S.; Hamilton, A. D. *Angew. Chem., Int. Ed. Engl.* **1997**, *36*, 2680−2683. (b) Park, H. S.; Lin, Q.; Hamilton, A. D. *J. Am. Chem. Soc.* **1999**, *121*, 8−13. (c) Blaskovich, M. A.; Lin, Q.; Delarue, F. L.; Sun, J.; Park, H. S.; Coppola, D.; Hamilton, A. D.; Sebti, S. M. *Nature Biotechnol.* **2000**, *18*, 1065−1070. (d) Jain, R. K.; Hamilton, A. D. *Angew. Chem., Int. Ed.* **2002**, *41*, 641−643.

(36) (a) Meissner, R.; Garcias, X.; Mecozzi, S.; Rebek, J., Jr. *J. Am. Chem. Soc.* **1997**, *119*, 77−85. (b) Rivera, J. M.; Martín, T.; Rebek, J., Jr. *Science* **1998**, *279*, 1021−1023. (c) Shivanyuk, A.; Rebek, J., Jr. *J. Am. Chem. Soc.* **2003**, *125*, 3432−3433.

(37) (a) Stupp, S. I.; LeBonheur, V.; Walker, K.; Li, L. S.; Huggins, K. E.; Keser, M.; Amstutz, A. *Science* **1997**, *276*, 384−389. (b) Percec, V.; Ahn, C.-H.; Ungar, G.; Yeardley, D. J. P.; Möller, M.; Sheiko, S. S. *Nature* **1998**, *391*, 161−164. (c) Cornelissen, J. J. L. M.; Fischer, M.; Sommerdijk, N. A. J. M.; Nolte, R. J. M. *Science* **1998**, *280*, 1427−1430. (d) Hirschberg, J. H. K. K.; Brunsveld, L.; Ramzi, A.; Vekemans, J. A. J. M.; Sijbesma, R. P.; Meijer, E. W. *Nature* **2000**, *407*, 167−170.

(38) (a) Olenyuk, B.; Whiteford, J. A.; Fechtenkotter, A.; Stang, P. J. *Nature* **1999**, *398*, 796−799. (b) Olenyuk, B.; Levin, M. D.; Whiteford, J. A.; Shield, J. E.; Stang, J. P. *J. Am. Chem. Soc.* **1999**, *121*, 10434−10435. (c) Orr, G. W.; Barbour, L. J.; Atwood, J. L. *Science* **1999**, *285*, 1049−1052. (d) Takeda, N.; Umemoto, K.; Yamaguchi, K.; Fujita, M. *Nature* **1999**, *398*, 794−796. (e) Caulder, D. L.; Raymond, K. N. *Acc. Chem. Res.* **1999**, *32*, 975−982.

(39) Wu, H.; Thalladi, V. R.; Whitesides, S.; Whitesides, G. M. *J. Am. Chem. Soc.* **2002**, *124*, 14495−14502.

(40) For a recent review on DNA compaction and condensation, see: Yoshikawa, K.; Yoshikawa, Y. In *Pharmaceutical Perspectives of Nucleic Acid-Based Therapeutics*; Mahato, R. I., Kim, S. W., Eds.; Taylor & Francis: London and New York, 2002; Chapter 8, pp 136−163.